Polymer-Induced Inverse-Temperature Crystallization of Nanoparticles on a Substrate

Xue-Zheng Cao,[†] Holger Merlitz,[†,‡,*] Chen-Xu Wu,[‡,*] and Jens-Uwe Sommer[†,§]

[†]Leibniz-Institut für Polymerforschung Dresden, 01069 Dresden, Germany, [‡]Department of Physics and ITPA, Xiamen University, Xiamen 361005, People's Republic of China, and [§]Institute of Theoretical Physics, Technische Universität Dresden, D-01069 Dresden, Germany

ABSTRACT Using molecular dynamics simulations, we study the properties of liquid state polymer–nanoparticle composites confined between two parallel substrates, with an attractive polymer–substrate interaction. Polymers are in the semidilute regime at concentrations far above the overlap point, and nanoparticles are in good solvent and without enthalpic attraction to the substrates. An increase of temperature then triggers the crystallization of nanoparticles on one of the two substrate surfaces—a surprising phenomenon, which is explained in terms of scaling theory, such as through competing effects of adsorption—and correlation blobs. Moreover, we show that the first, closely packed layer of nanoparticles on the substrate increases the depletion attraction of additional nanoparticles from the bulk, thereby enhancing and stabilizing the formation of a crystalline phase on the substrate. Within the time frame accessible to our numerical simulations, the crystallization of nanoparticles was irreversible; that is, their crystalline phase, once created, remained undamaged after a decrease of the temperature. Our study leads to a class of thermoreactive nanomaterials, in which the transition between a homogeneous state with dissolved nanoparticles and a surface-crystallized state is triggered by a temperature jump.

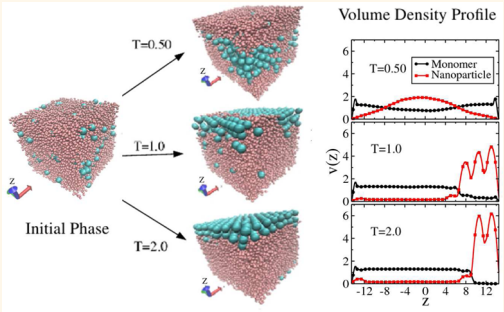

KEYWORDS: polymer · nanoparticle · crystallization · depletion · adsorption · correlation

Polymer–nanoparticle composites exhibiting advantageous electrical, optical, and mechanical applications are of interest for chemical sensors, flexible solar cells, self-healing, and high-performance electronics.[1] The availability of nanoparticles of various sizes and diverse chemical properties opens up the possibility of imparting anticipated functionality to composite materials. Clarifying the mechanisms by which nanoparticles interact with polymers is a prerequisite for designing polymer–nanoparticle composites, thereby combining useful properties of both polymers and nanoparticles.[2] It enriches the understanding of the relationship between nanoscale property and mesoscope structure. In general, the phase behavior of polymer–nanoparticle composites is governed by an intricate balance of entropic and enthalpic interactions.[3−5]

The presence of an additional surface can significantly alter the phases that are developed in bulk polymer–nanoparticle composites.[6] By way of simulations and experiments, it has been found that nanoparticles are often driven to a substrate or into defects, which exist in the substrate material upon annealing.[7,8] The forces acting on the nanoparticles are predominately of entropic origin when the polymers and nanoparticles are chemically similar. By using classical density functional theory (DFT), Mackay and co-workers concluded that there exists a first-order phase transition, induced by entropic interactions, in which the nanoparticles segregate to the substrate and form a densely packed monolayer above a certain nanoparticle density, expelling the polymers away from the substrate surface.[9,10] Recently, the same authors showed that adding attractions between polymers and the substrate had an effect of delaying and even suppressing the segregation transition.[11] Therefore, the aggregation behavior of nanoparticles on the substrate surface depends on the entropy related to polymer conformation, as well as on the enthalpy resulting from the attraction between polymers and the substrate. Inspired by these considerations, in this work, we focus on

* Address correspondence to merlitz@gmx.de, cxwu@xmu.edu.cn.

Received for review July 22, 2013 and accepted October 1, 2013.

Published online October 07, 2013
10.1021/nn4037738

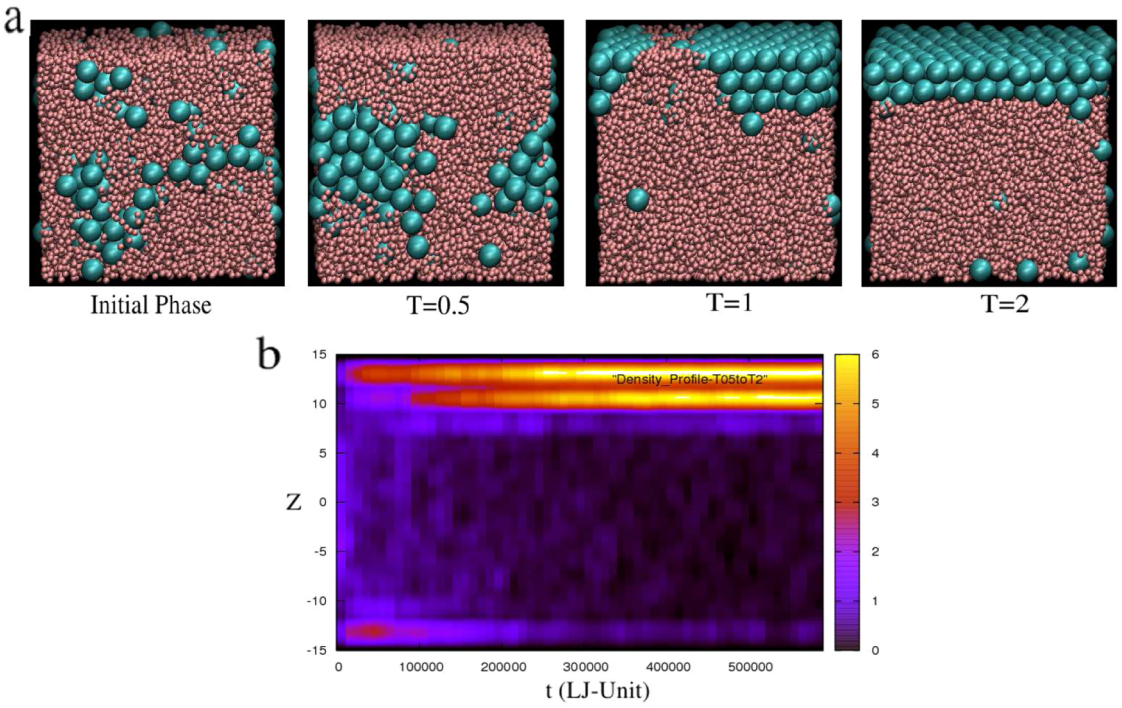

Figure 1. Polymer–nanoparticle composite in confinement: (a) snapshots of equilibrium phases at different temperatures (substrates confining the top and the bottom are not shown); (b) time evolution of the volume density profile of nanoparticles, perpendicular to the substrate surfaces, after the system was heated up from $T = 0.5$ to $T = 2.0$. Color contours indicate local volume fractions of nanoparticles over their bulk value. Bulk polymer volume fraction, $c = 0.257$; bulk nanoparticle volume fraction, $c_{NP} = 0.146$; attraction strength between monomers and substrate, $\varepsilon = 0.2$.

polymer–nanoparticle composites confined between two parallel substrates. The computer simulations revealed that the nanoparticles, forming irregular clusters at low temperatures, assume a higher degree of order at higher temperatures while creating crystalline layers on one of the substrates. The polymer-induced effective interactions between nanoparticle–substrate and among nanoparticles, being responsible for the inverse temperature crystallization of nanoparticles, are discussed for systems of varying polymer concentration and monomer–substrate interaction.

RESULTS AND DISCUSSION

Behaviors of Confined Polymer–Nanoparticle Composites upon Increasing Temperature. In a first series of simulations, the volume fractions of polymers and nanoparticles were kept constant at $c = 0.257$ and $c_{NP} = 0.146$, respectively. The polymer concentration was well above the overlap threshold ($c^* \approx 0.05$) and below the melt density.[12] After a relaxation inside a simulation box with periodic boundaries, nanoparticles and polymers were distributed fairly homogeneously inside the system. The resulting conformation was taken as the initial phase for further studies. Two parallel LJ walls, serving as the confining substrates, were added, and these walls had an attractive interaction with the monomers of strength $\varepsilon = 0.2$ (see eq 3). Upon relaxation of the system at low temperature, $T = 0.5$, polymers were (as a result of their attraction to the substrates) adsorbed on both surfaces, while the nanoparticles aggregated in the central region of the film, as shown in Figure 1a. Note that in this case a partial solidification of the nanoparticles is visible, which is not seen in the case of the fully periodic system, and is triggered by the confining substrates which effectively increase the inter-nanoparticle depletion attraction.[13]

An increase of the temperature then led to a segregation of the nanoparticles at the substrate surface, which tend to crystallize on just one of the two substrates. The fraction of nanoparticles segregated at the surface is further enlarged at higher temperatures. As shown in the snapshot at $T = 2.0$ (Figure 1a), the substrate surface is completely covered with nanoparticles, arranged in a hexagonal packing. For systems studied in the present paper, the distance between the walls is about 1 order of magnitude larger than the radius of gyration of the polymer chains. In this case, confinement does not affect the depletion attraction and thereby the crystallization of nanoparticles. Therefore, similar behavior is expected on a single surface. Starting from an amorphous phase in which nanoparticles and polymers are mixed in bulk, such as an equilibrium state at $T = 0.5$, the crystallization of nanoparticles takes place quite rapidly when the temperature is increased to $T = 2.0$, as can be seen in Figure 1b, in which we have plotted the time evolution of the density profile after the temperature jump. In what follows, we will explain the origin of this behavior.

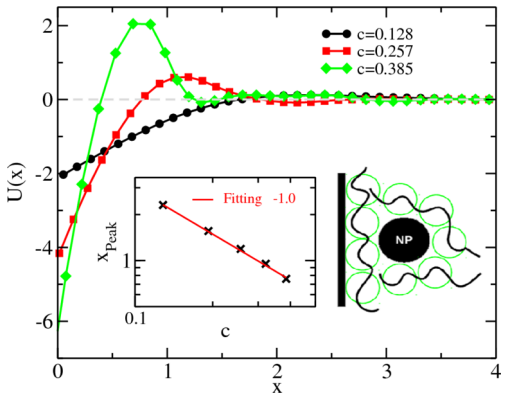

Figure 2. Effective athermal polymer-induced entropic depletion potential between one nanoparticle and a substrate at increasing polymer concentrations. The sketch shows a simplified conceptual model in which the polymer matrix is represented as a melt of correlation blobs (in green). A fit of the correlation blob size as function of polymer concentration is shown in the inset.

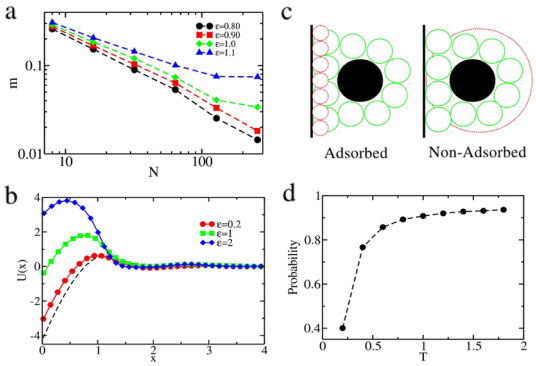

Figure 3. (a) Adsorption probability of monomers of one single chain with one end grafted on the substrate as function of chain length for different monomer−substrate attractions. (b) Computed effective potentials between one nanoparticle and a substrate, induced by attractive polymers at different monomer−substrate attractions; the dotted line shows the corresponding entropic depletion potential, here c = 0.257 and T = 1.0. (c) Sketches of correlation blobs (in green) being adsorbed and desorbed; the adsorption blobs are shown in red. (d) Fraction of nanoparticles adsorbed on a substrate as a function of temperature at constant monomer−substrate attraction, here c = 0.257, c_{NP} = 0.0271, and ε = 0.2.

Entropic Depletion. In a previous study about the effective interaction between two nanoparticles immersed in an athermal polymer solution, we had verified that the depletion forces induced by athermal polymers were well-described with a scaling model in which the attraction between particles is caused by the depletion of correlation blobs.[14] In a similar way, we directly calculated the entropic depletion forces between one nanoparticle and a hard wall at different polymer concentrations. The corresponding potentials are shown in Figure 2. Here, the density of polymer matrix was varied between c = 0.128 and c = 0.385, above the overlap concentration of $c^* \approx 0.05$ for chains of length N = 64. The depletion attraction is intensified at increasing polymer concentration, and a repulsive barrier is observed. In combination with the knowledge that the conformation of athermal polymers on length scales smaller than the correlation length is not disturbed by a hard substrate,[15] we assume that polymers close to the substrate are represented by correlation blobs in the same way as in the vicinity of the particle, and the substrate surface can be considered as a particle of infinite size. When the nanoparticle approaches the substrate, it has to squeeze out the correlation blobs located between, as shown in the sketch of Figure 2. The repulsive barrier then emerges in analogy to the depletion potential induced by unconnected monomers.[16]

The corresponding peak position x_{peak} of each depletion potential, as a function of polymer concentration c, is plotted and fitted with a power law, yielding $x_{peak} \sim c^{-1}$, as shown in the inset of Figure 2. This is consistent with the assumption that, once the concentration is well above overlap and the correlation blob size correspondingly small, it approaches the order of the thermal blob size,[17−19] and hence, despite of being in good solvent, the dominating scaling contribution to ξ turns proportional to c^{-1}. The depletion potential can be estimated to be of the order of kT for each correlation blob being squeezed out of the region between the nanoparticle and the substrate.

In the Presence of Monomer−Substrate Attraction. The addition of an attractive interaction between polymers and the substrates increases the number of monomers in contact with the substrate surfaces, which are thereby gaining adsorption energy. Hence, the conformation of the polymers is obtained from the balance between the attractive energy which tends to bring the polymers on the surface and the corresponding loss in entropy. There exists a critical contact energy ε_{cr} between monomers and the substrate surface,[20,21] which corresponds to the adsorption transition in the dilute system. A single polymer chain is adsorbed when the attraction strength between monomers and the substrate surface exceeds the critical value, $\varepsilon > \varepsilon_{cr}$. To estimate the value of ε_{cr} for polymer chains simulated here, we have computed the adsorption probability m of monomers of a single polymer chain with one end grafted on the substrate as a function of polymer chain length N and varying monomer−substrate attractions.

Based on a scaling analysis,[21] at $\varepsilon > \varepsilon_{cr}$, there exists a finite probability, the value of which depends on the monomer−substrate attraction strength, for monomers of one long chain to be adsorbed on the substrate surface. Otherwise, if $\varepsilon < \varepsilon_{cr}$, this probability asymptotically approaches zero for long chains according to $m \sim 1/N$. Figure 3a implies that $\varepsilon_{cr} \approx 0.95 \pm 0.05$ for the bead spring model used in this work. There exists a characteristic adsorption thickness ξ_{ads} for a single polymer chain near the substrate surfaces for $\varepsilon > \varepsilon_{cr}$: On length scales smaller than that, the attractive interaction is weaker than the thermal energy and the

chains remain in an unperturbed conformation. In scaling theory, this layer of polymers is considered to be made of adsorption blobs, the size of which scales as $\xi_{ads} \sim (kT)/(\varepsilon - \varepsilon_{cr})$.[21−23] On average, chain sections of the size of the adsorption blob are attracted to the substrate surface with an energy of the order of kT. The adsorption blob size is decreasing rapidly in the small interval of the monomer−substrate attraction strength ε, once it is above its critical ε_{cr}. A calculation of the radius of gyration of a single, long chain ($N = 512$), in the direction perpendicular to the substrate surface, shows that $R_{gz} \approx 0.52$ when $\varepsilon = 2.0$.

In semidilute solution, the effect of the surface is screened out at distances larger than the bulk correlation length ξ.[21−23] Polymers are therefore adsorbed on the substrate surface if ξ_{ads} is smaller than the bulk correlation length. In this case, it is assumed that only those monomers inside a correlation length are adsorbed and the whole chain consists of adsorbed sections which are in random contact with the surface, in marked contrast to the flatly adsorbed state of an isolated chain. This situation is sketched in Figure 3c: For $\xi > \xi_{ads}$, if the nanoparticle approaches the substrate surface, the enthalpic contribution of a single correlation blob is stronger than the entropic contribution gained during a depletion of the correlation blob from the surface. On the other hand, the crossover from the adsorbed to the non-adsorbed state takes place when the adsorption blob turns larger than the correlation blob, $\xi_{ads} > \xi$. See the right sketch of Figure 3c, where the surface attraction is insufficient for the correlation blobs to be adsorbed.

The effective interactions between one nanoparticle and a substrate at different monomer−substrate attraction strengths are shown in Figure 3b. Compared to the polymer-induced entropic depletion potential (dotted line), the depletion attraction at short range is largely eliminated for $\varepsilon \approx \varepsilon_{cr}$ and turning into a repulsion when $\varepsilon = 2$ because the monomers are then strongly attached to the substrate. Note that an extended attractive tail, exterior to the short-range repulsion, which is found with nanoparticle pairs in the presence of attraction between polymers and nanoparticles,[12] is not observed here. This is because the nanoparticle is not enthalpically "dressed" by monomers. For $\varepsilon \ll \varepsilon_{cr}$, the enthalpic contribution of the monomer−substrate attraction to one correlation blob on the substrate surface cannot compete with the gain of entropy related to a squeeze out of the correlation blob. The corresponding potential in Figure 3b shows that the entropic depletion effect is dominant for $\varepsilon = 0.2$. However, even in case of larger adsorption blobs, $\xi_{ads} > \xi$, there is still a decrease observable in the free energy of a correlation blob in contact with the substrate, which lowers the depletion attraction.

In practice, it is usually easier to modify the system temperature than to fine-tune the surface property of the substrate (or to change the solvent properties) in order to adjust the strength of attraction between substrate and polymers. As the temperature increases, the adsorption correlation length is enlarged and the area density of adsorption blobs is reduced. Eventually, the entropic depletion attraction between the nanoparticles and the substrate is sufficiently high to replace the adsorbed polymers, and the osmotic pressure which is driving the nanoparticles toward the substrate overcomes the enthalpic attraction of the polymers. In Figure 3d, we show that the probability of nanoparticles to be adsorbed on the substrate is enhanced by an increase of the temperature when ε is fixed.

Irreversible Crystallization. For those nanoparticles that are depleted at the substrate, there exist polymer-induced depletion forces of two-body as well as of three-body type, the latter acting in the direction parallel to the substrate surface, as shown in the top panel of Figure 4a. Once a closed layer of nanoparticles is developed on one of the two substrates, a depletion attraction (see bottom figure of Figure 4a) emerges between the layer made of nanoparticles and a nanoparticle in bulk. This depletion attraction is far stronger than the depletion potential induced between a nanoparticle and the bare substrate. This can be explained by a key-lock principle since the nanoparticles fit exactly into the preordered structure of the already existing layer, and thus the depletion effect is maximized. As a result, once a closed layer of nanoparticles is formed at one of the substrates, this side displays an enhanced nucleation of the second layer. Consequently, the crystallization of nanoparticles takes place preferentially on one of the two substrates.

Our simulations thus indicate that the crystalline phase is rather stable with respect to a decrease of temperature, and the system displays a pronounced hysteresis. In Figure 4b, the time evolution of the nanoparticle density profile is shown, this time starting with a pre-existing crystalline double layer of particles at $T = 2$. After a decrease of the temperature back to $T = 0.5$ (top panel), the layer does not break up, as might be expected, but instead stays on. We point out that this simulation covered a far longer time than that previously required for the amorphous nanoparticles to crystallize. The strong depletion attraction among the nanoparticles, as discussed above in Figure 4a, supports the assumption that the crystallized nanoparticles are trapped in a metastable state by the surrounding polymers. The enthalpic interaction between the polymers and the substrate are of short range and effectively shielded by the closed nanoparticle layer. Note that the depletion attraction within the NP layer is always controlled by athermal monomer−NP interactions, which stabilizes the crystalline phase once it has nucleated at the surface. To reverse the nanoparticle depletion, the polymer would have to penetrate into

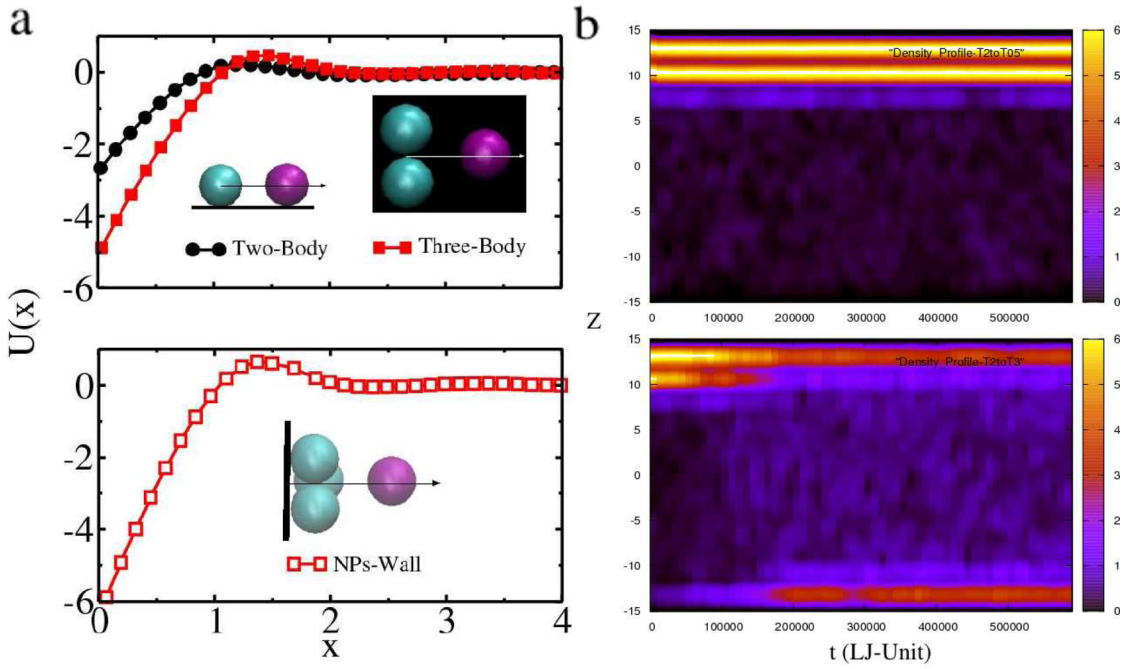

Figure 4. (a) Polymer-induced two- and three-body effective interactions between nanoparticles in contact with a substrate, and the effective interaction between one nanoparticle in bulk and a closed layer made of nanoparticles adsorbed on the substrate surface (lower); $c = 0.257$ and $\varepsilon = 0.2$. (b) Evolution of the volume density profiles of the nanoparticles: Starting at $T = 2.0$ and running at low temperature $T = 0.5$ (top panel) and even higher temperature $T = 3.0$ (bottom panel); $c = 0.257$, $c_{NP} = 0.146$, and $\varepsilon = 0.2$.

the layer and repel some of the nanoparticles, which requires overcoming a free energy barrier. Of course, the crystal structure of nanoparticles can be molten when further increasing the temperature to higher values, as shown in the lower part of Figure 4b, in which the temperature was increased to $T = 3$. The depletion attraction between the substrate and the nanoparticles is of entropic nature, and thus even in the quasi-athermal case, a large number of nanoparticles are located near the substrate surface. At very high temperature, however, some nanoparticles can escape trapping between bulk polymers and the substrate due to enhanced thermal fluctuation and the gain in translational entropy. This might be considered as a partial re-entry transition toward a molten state of nanoparticles. The melting point is near $T_{melt} \approx 2.75$ for the sample investigated here.

CONCLUSIONS

Polymer–nanoparticle composites confined between two substrates have been studied using molecular dynamics simulations. Depletion forces between nanoparticles and the substrate and between nanoparticles have been calculated using a sampling method in which a given nanoparticle is fixed using a harmonic spring. We considered the case in which the polymer matrix interacted with the substrates but not with the nanoparticles. In this way, we could switch between a surface-crystallized state and a bulk state of nanoparticles. A potential experiment of polymer-mediated and temperature-controlled assembly of nanoparticles could be done by adding polymer–nanoparticle composites on a chemically desired solid surface with attractive interaction to polymers. The polymer-induced inverse temperature crystallization of nanoparticles is expected to lead to applications in the design of advantageous nanomaterials.[24–26]

The entropic depletion attraction between nanoparticles and a substrate is responsible for the adsorption of nanoparticles on the substrate surface. It leads to a gain in free energy of the order of 1 kT for each correlation blob that was squeezed out of the region between the particle and the substrate. Adding an attractive interaction between polymers and the substrate has an effect of weakening this depletion attraction, which thus can be turned into a repulsion when the monomer–substrate attraction strength is sufficiently strong. In this case, the entropic energy gain during the depletion of one correlation blob from the substrate is lower than the accumulative enthalpic contribution of polymer sections of the correlation blob which are in contact with the surface. Reducing the monomer–substrate attraction strength or enhancing the system temperature increases the adsorption correlation length. Monomers on the surface are replaced by nanoparticles if the size of the adsorption blob, ξ_{ads}, is larger than the correlation blob of the semidilute polymer matrix.

For those nanoparticles in contact with the surface of the substrate, polymer-induced depletion forces of

two-body as well as of three-body type tend to pack them in the direction parallel to the substrate surface, leading to the ordering aggregation of nanoparticles. The depletion attraction between a closed layer of nanoparticles and a nanoparticle in bulk is of far stronger quantity than the force induced between a nanoparticle and a bare substrate since here a nanoparticle fits exactly into the preordered structure formed by the other nanoparticles. As a result, once a closed layer of nanoparticles is formed at one of the two substrates, this side displays enhanced nucleation of nanoparticles for the second layer.

SIMULATION METHODS

Model. In our simulations, the polymers with chain length $N = 64$ were modeled as bead spring chains without explicit twisting or bending potential. Each chain consisting of monomers was connected by anharmonic springs, modeled with a finite extensible nonlinear elastic (FENE) potential[27]

$$U_{\mathrm{FENE}}(r) = -0.5\kappa R_0{}^2 \ln\left[1 - \left(\frac{r}{R_0}\right)^2\right], r < R_0 \quad (1)$$

where $\kappa = 30\varepsilon/\sigma_M{}^2$ is the spring constant, $\varepsilon = 1$, and $R_0 = 1.5\sigma_M$ is the maximum pair length to prohibit the interaction of chains. Here, $\sigma_M = 1$ stands for the monomer size, and nanoparticle size is fixed at constant $\sigma_{NP} = 3$. The interactions between particles (including nanoparticle−nanoparticle, nanoparticle−monomer, and monomer−monomer) were modeled as Lennard-Jones (LJ) potentials

$$U_{\mathrm{LJ}}(r) = 4\left(\left(\frac{\sigma_{ij}}{r}\right)^{12} - \left(\frac{\sigma_{ij}}{r}\right)^{6}\right) \quad (2)$$

cut at its minimum $r_{\min} = 2^{1/6}\sigma_{ij}$, $U_{\mathrm{LJ}}(r) = 0$ when $r > r_{\min}$, with σ_{ij} being the mean size of the two particles (ith and jth) involved in the pair interaction. In addition, a LJ potential

$$U_{\mathrm{Wall}}(x) = 4\varepsilon\left(\left(\frac{\sigma_i}{x+\sigma_i}\right)^{12} - \left(\frac{\sigma_i}{x+\sigma_i}\right)^{6}\right) \quad (3)$$

was implemented between the two substrates at positions $z = -15$ and $z = 15$ and the particles to deliver a confinement effect. Here $\sigma_i = \sigma_{NP}$ for nanoparticles and $\sigma_i = \sigma_M$ for monomers, x being the closest surface distance between the substrate and the ith particle involved in the interaction. In the case of polymer−nanoparticle composites confined between two attractive substrates, the monomer's LJ−wall interaction with the substrates is cut at $2.5\sigma_M$, while the same interaction between nanoparticle and substrate is cut at its minimum, $x_{\min} = 2^{1/6}\sigma_{NP} - \sigma_{NP}$, so that $U_{\mathrm{Wall}}(x) = 0$ when $x > x_{\min}$. In this case, there is an excess attractive energy gain ε for each monomer close to the substrates. To simulate athermal systems, both the LJ−wall interactions between monomer−wall and nanoparticle−wall are cut at its minimum. The boundary conditions in both x and y directions are periodic to mimic an infinitely extended film-like geometry. The simulations are carried out using the open source LAMMPS molecular dynamic package.[28] The equation of motion for the displacement of particle with index i is given by the Langevin equation:

$$m_i \frac{d^2\mathbf{r}_i}{dt^2} = -\nabla_i U - m_i\Gamma\frac{d\mathbf{r}_i}{dt} + \mathbf{W}_i(t) \quad (4)$$

where U is the total potential energy acting on the ith particle, for monomer $U = U_{\mathrm{LJ}} + U_{\mathrm{FENE}} + U_{\mathrm{Wall}}$, and for nanoparticle $U = U_{\mathrm{LJ}} + U_{\mathrm{Wall}}$. The quantity $\mathbf{W}_i(t)$ is a stochastic force that is related to the friction coefficient by the fluctuation−dissipation theorem.[29]

Every simulation was carried out at a certain constant temperature in a cubic box of size $d = 30$. Throughout the paper, the volume ratio $c = N_{\mathrm{Monomer}}\pi\sigma_M^3/6d^3$ was used to define the polymer concentration, N_{Monomer} being the number of monomers inside the system. Correspondingly, $c_{NP} = N_{NP}\pi\sigma_{NP}^3/6d^3$ was used to define the nanoparticle concentration, where N_{NP} is the number of nanoparticles inside the system. Each system was initially relaxed in a simulation of 8×10^8 timesteps (corresponding to 8×10^5 LJ times).

Force Calculation. In order to calculate polymer-induced effective forces between one nanoparticle and a substrate, we bind the nanoparticle at a distance r_0 from the substrate. A stiff harmonic spring potential acting on the nanoparticle, $f_{\mathrm{spring}}(r) = -k(r - r_0)$ with $k = 150$, was used to enforce a well-defined average distance r over a large number of timesteps for each choice of r_0. The average distance r was then used to measure the effective force acting on the nanoparticle.[12,14] More specifically, the equation

$$f_{\mathrm{spring}}(\bar{r}) + f_{\mathrm{effective}}(\bar{r}) = 0 \quad (5)$$

was used, where $f_{\mathrm{effective}}$ denotes the effective force induced by the surrounding polymer matrix. In eq 5, we have expressed the force as a function of the average distance, instead of using ensemble-averaged forces. Since the fluctuations about r_0 remained very small, both approaches delivered identical results within the accuracy achieved in the simulations. In order to measure the depletion force as a function of particle separation, $f_{\mathrm{effective}}$, the value of r_0 was varied in separate simulations. Once the depletion forces were determined, the corresponding potential U_{eff} was obtained through integration.

Conflict of Interest: The authors declare no competing financial interest.

Acknowledgment. This work has been supported by the European Union (ERDF) and the Free State of Saxony *via* TP A2 ("MolDiagnostik") of the Cluster of Excellence "European Center for Emerging Materials and Processes Dresden" (ECEMP) and was partly supported by the National Science Foundation of China under Grant Nos. 11074208 and 11274258 and by the DFG priority program SPP 1369.

REFERENCES AND NOTES

1. Balazs, A. C.; Emrick, T.; Russell, T. P. Nanoparticle Polymer Composites: Where Two Small Worlds Meet. *Science* **2006**, *314*, 1107–1110.
2. Balazs, A. C. Nanocomposites: Economy at the Nanoscale. *Nat. Mater.* **2007**, *6*, 94–95.
3. Mackay, M. E.; Tuteja, A.; Duxbury, P. M.; Hawker, C. J.; Horn, B. V.; Guan, Z.; Chen, G.; Krishnan, R. S. General Strategies for Nanoparticle Dispersion. *Science* **2006**, *311*, 1740–1743.
4. Krishnan, R. S.; Mackay, M. E.; Duxbury, P. M.; Pastor, A.; Hawker, C. J.; Horn, B. V.; Asokan, S.; Wong, M. S. Self-Assembled Multilayers of Nanocomponents. *Nano Lett.* **2007**, *7*, 484–489.
5. Stamm, M.; Sommer, J. U. Polymer−Nanoparticle Films: Entropy and Enthalpy at Play. *Nat. Mater.* **2007**, *6*, 260–261.
6. Böltau, M.; Walheim, S.; Mlynek, J.; Krausch, G.; Steiner, U. Surface-Induced Structure Formation of Polymer Blends on Patterned Substrates. *Nature* **1998**, *391*, 877–879.
7. Tyagi, S.; Lee, J. Y.; Buxton, G. A.; Balazs, A. C. Using Nanocomposite Coatings To Heal Surface Defects. *Macromolecules* **2004**, *37*, 9160–9168.
8. Gupta, S.; Zhang, Q.; Emrick, T.; Balazs, A. C.; Russell, T. P. Entropy-Driven Segregation of Nanoparticles to Cracks in Multilayered Composite Polymer Structures. *Nat. Mater.* **2006**, *5*, 229–233.
9. McGarrity, E. S.; Frischknecht, A. L.; Frink, L. J. D.; Mackay, M. E. Surface-Induced First-Order Transition in Athermal

Polymer−Nanoparticle Blends. *Phys. Rev. Lett.* **2007**, *99*, 238302.
10. McGarrity, E. S.; Frischknecht, A. L.; Mackay, M. E. Phase Behavior of Polymer/Nanoparticle Blends near a Substrate. *J. Chem. Phys.* **2008**, *128*, 154904–154903.
11. Frischknecht, A. L.; Padmanabhan, V.; Mackay, M. E. Surface-Induced Phase Behavior of Polymer/Nanoparticle Blends with Attractions. *J. Chem. Phys.* **2012**, *136*, 164904–164916.
12. Cao, X. Z.; Merlitz, H.; Wu, C. X.; Egorov, S. A.; Sommer, J. U. Effective Pair Potentials between Nanoparticles Induced by Single Monomers and Polymer Chains. *Soft Matter* **2013**, *9*, 5916–5926.
13. Spannuth, M.; Conrad, J. C. Confinement-Induced Solidification of Colloid-Polymer Depletion Mixtures. *Phys. Rev. Lett.* **2012**, *109*, 028301.
14. Cao, X. Z.; Merlitz, H.; Wu, C. X.; Sommer, J. U. Polymer-Induced Entropic Depletion Potential. *Phys. Rev. E* **2011**, *84*, 041802.
15. Lekkerkerker, H. N. W.; Tuinier, R. *Colloids and the Depletion Interaction*; Springer: Dordrecht, Heidelberg, London, New York, 2011.
16. Crocker, J. C.; Matteo, J. A.; Dinsmore, A. D.; Yodh, A. G. Entropic Attraction and Repulsion in Binary Colloids Probed with a Line Optical Tweezer. *Phys. Rev. Lett.* **1999**, *82*, 4352–4355.
17. Schaefer, D. W.; Joanny, J. F.; Pincus, P. Dynamics of Semiflexible Polymers in Solution. *Macromolecules* **1980**, *13*, 1280–1289.
18. Verma, R.; Crocker, J. C.; Lubensky, T. C.; Yodh, A. G. Entropic Colloidal Interactions in Concentrated DNA Solutions. *Phys. Rev. Lett.* **1998**, *81*, 4004–4007.
19. Jun, S.; Arnold, A.; Ha, B. Y. Confined Space and Effective Interactions of Multiple Self-Avoiding Chains. *Phys. Rev. Lett.* **2007**, *98*, 128303.
20. De Gennes, P. G. Scaling Theory of Polymer Adsorption. *J. Phys. (Paris)* **1976**, *37*, 1445–1452.
21. Eisenriegler, E.; Kremer, K.; Binder, K. Adsorption of Polymer Chains at Surfaces: Scaling and Monte Carlo Analyses. *J. Chem. Phys.* **1982**, *77*, 6296–6320.
22. De Gennes, P. G.; Pincus, P. Scaling Theory of Polymer Adsorption: Proximal Exponent. *J. Phys. Lett.* **1983**, *44*, 241–246.
23. Bouchaud, E.; Daoud, M. Polymer Adsorption: Concentration Effects. *J. Phys. (Paris)* **1987**, *48*, 1991–2000.
24. Sun, S. H.; Anders, S.; Hamann, H. F.; Thiele, J. U.; Baglin, J. E. E.; Thomson, T.; Fullerton, E. E.; Murray, C. B.; Terris, B. D. Polymer Mediated Self-Assembly of Magnetic Nanoparticles. *J. Am. Chem. Soc.* **2002**, *124*, 2884–2885.
25. Shenhar, R.; Norsten, T. B.; Rotello, V. M. Polymer-Mediated Nanoparticle Assembly: Structural Control and Applications. *Adv. Mater.* **2005**, *17*, 657–669.
26. Kim, D. K.; Lai, Y. M.; Diroll, B. T.; Murray, C. B.; Kagan, C. R. Flexible and Low-Voltage Integrated Circuits Constructed from High-Performance Nanocrystal Transistors. *Nat. Commun.* **2012**, *3*, 1216.
27. Kremer, K.; Grest, G. S. Dynamics of Entangled Linear Polymer Melts: A Molecular-Dynamics Simulation. *J. Chem. Phys.* **1990**, *92*, 5057–5086.
28. Plimpton, S. Fast Parallel Algorithms for Short-Range Molecular Dynamics. *J. Comput. Phys.* **1995**, *117*, 1–19.
29. Dünweg, B.; Paul, W. Brownian Dynamics Simulations without Gaussian Random Numbers. *Int. J. Mod. Phys. C* **1991**, *02*, 817–827.